SUBBAND KALMAN FILTERING WITH APPLICATIONS TO TARGET TRACKING

P. De Leon[1], *W. Kober*[2], *K. Krumvieda*[2], *J. Thomas*[2]

[1]New Mexico State University
Klipsch School of Electrical Engineering
Las Cruces, New Mexico 88003-8001, USA

[2]Data Fusion Corp.
10190 Bannock St., Suite 246
Northglenn, Colorado 80234, USA

ABSTRACT

The Kalman filter has been successfully applied to target tracking. However, the Kalman filter is computationally demanding if the input measurement rate is high and/or if the state dimension is large. Furthermore, noisy measurements may decrease Kalman filter tracking accuracy. One way to possibly reduce the computational rate and sensitivity to noisy measurements is to partition the input spectrum into subbands, downsample, and employ Kalman filters in each subband. In this paper we present the relations of subband Kalman filter inputs and outputs to their fullband counterparts. We also present results from the target-tracking application which demonstrate the subband implementation performs equal to or better (in terms of error variance) than the fullband case when 1) only subband Kalman filters with significant energy are updated and 2) when the measurement noise is large.

1. INTRODUCTION

Multiresolutional approaches have been employed in signal processing (time domain), image processing (spatial domain) and computer vision (time and/or spatial domains) to achieve performance which cannot be realized using conventional, single-resolution, processing [1]. Multirate techniques have been used for many years for many advantages, such as reduced computational complexity for a given task, reduced transmission rates and/or reduced storage requirements depending on the application [2]. The application of these techniques to target tracking has been explored by Hong [3], [4], [5], [6], who considers both spatial resolution reduction (multiresolution tracking) and temporal resolution (multirate tracking) in his work. In [10] an algorithm of multirate interacting multiple model (MRIMM) was developed. The MRIMM algorithm can be used instead of the conventional IMM to yield a nearly equivalent performance (or a better performance when targets do not exhibit maneuvering behaviors) at significant computational savings.

Implicit to the concept of multirate tracking is the assumption that the sensor update rate is determined by a desire to maintain tracking on multiple targets through a predefined maneuver envelope. The resulting sampling rate, then, will be based on the most extreme maneuver, considerably higher than is necessary to maintain a target track under more benign maneuver conditions. Because of the oversampling, the sensor measurement stream can be compressed with little or no degradation in tracker performance. The compression is implemented by the multirate tracking (MRT) algorithm, which provides for tracking operations at any number of update rates. The correct update rate can be determined by multiple-model filtering which provides an estimate of the target maneuver condition and, indirectly, the necessary update rate to maintain track quality.

Multirate target tracking entails transformation of both the incoming measurements as well as the model of the target being tracked [3]. The result of these transformations is a series of data streams representing noise-corrupted measurements of the target available at various rates, as well as an appropriate linear model tuned to each sampling period. Tracking, then, can be performed at any level of this measurement tree. The highest-rate data stream is the original unprocessed sensor measurement sequence, and exhibits all of the properties of the original problem. The lower-rate levels of the measurement tree require less computing power to process as well as exhibiting lower equivalent measurement noise (for perfect association) because each low-rate measurement is, in fact, a composite representation of several full-rate measurements. Multiresolution processing can be analogously applied, resulting in a complete matrix of measurement sequences and models, each of varying resolutions and update rates and each implying a different target model. Several conventional tracking algorithms were implemented by in this data framework and demonstrated equivalent or superior performance while yielding significant computational savings [4].

While previous approaches have employed a wavelet decomposition (Haar basis functions), this work examines the use of a filter bank decomposition (uniform frequency bands). Unlike previous approaches, we employ filters which more carefully isolate frequency components and oversampled subbands which minimize subband aliasing and its effect on the track estimate. In addition, the subband approach leads to signal components with identical sampling rates and possibly a simpler parallel processing implementation [7]. In this paper we present the relations of subband Kalman filter inputs/outputs and filterbank components to their fullband counterparts.

Results from the application of the subband Kalman filter to target tracking is compared to the fullband equivalent.

2. SUBBAND KALMAN FILTER INPUT/OUTPUT EQUATIONS

2.1 Background

In target tracking, three coupled 3-state Kalman filters are used for estimation of states [8]. The states or modes are given by

$$R, \dot{R}, \ddot{R}, \theta, \dot{\theta}, \ddot{\theta}, \phi, \dot{\phi}, \ddot{\phi} \tag{1}$$

where R is range, θ is azimuth, and ϕ is elevation. These are arranged into the state vectors

$$\begin{aligned} \mathbf{x}_R &= \begin{bmatrix} x_R & x_{\dot{R}} & x_{\ddot{R}} \end{bmatrix}^T \\ \mathbf{x}_\theta &= \begin{bmatrix} x_\theta & x_{\dot{\theta}} & x_{\ddot{\theta}} \end{bmatrix}^T \\ \mathbf{x}_\phi &= \begin{bmatrix} x_\phi & x_{\dot{\phi}} & x_{\ddot{\phi}} \end{bmatrix}^T \end{aligned} \tag{2}$$

For each subband Kalman filter, the measurement vector **y** is decomposed by first forming a vector time-series of the measurement data and then analysis filtering and downsampling. The subband versions of the transition matrix $\mathbf{\Phi}$, noise covariance associated with the transition matrix **Q**, observation matrix **H**, and the noise covariance associated with the observation matrix $\mathbf{R}_c$ are updated in the Kalman recursion. After subband Kalman filtering, we synthesize the fullband state vector estimate $\hat{\mathbf{x}}$ [9]. The block diagram for the subband Kalman filter system is shown in Figure 1.

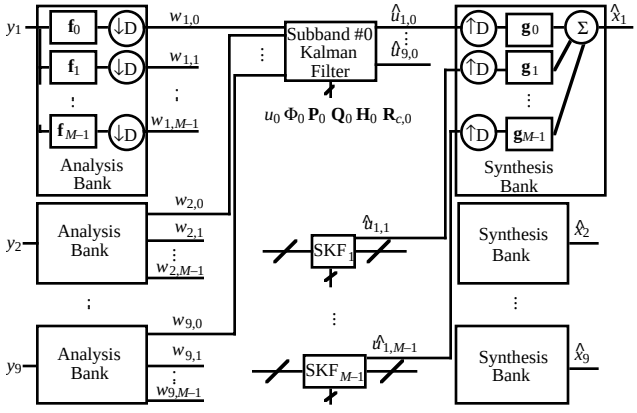

Figure 1: Subband Kalman filter.

Due to the various matrix multiplications and inversions, the Kalman filter is a demanding application for real-time signal processing especially if the input data (measurement) rate is high and/or if the state dimension is large. Previous work in MR target tracking has exclusively employed wavelet decompositions (not uniform subband decompositions) and shown some benefits at the expense of increased computation [4]. In performing Kalman filtering in subbands for the target tracking application, we may realize the following benefits:

- By performing the filtering in subbands, we can more effectively track maneuvers given low SNR measurements as compared to fullband implementations.
- We have the option of selectively updating subband Kalman filters thereby reducing computational cost as well as computing the updates in parallel.

In order to mitigate the effects of subband aliasing, we employ oversampled subbands (at the expense of increased computation) since subband aliasing associated with critically-sampled subbands (and similarly wavelets) substantially reduces the performance in the Kalman filter.

One concern in using subband Kalman filtering for tracking is the delay involved in the subband decomposition. This delay, however, can be controlled in the analysis/synthesis filter design. Additionally, in the case where high-rate sensor data is short-time averaged before lower-rate processing, the high-rate sensor data can simply be directed to the filterbank for immediate subband processing thereby equalizing the delay imposed by averaging (in the fullband case) and the filter bank (in the subband case).

2.2 Target Tracking using the Kalman Filter

In the presentation of the input/output equations for the subband Kalman filter, we assume M subbands indexed by m; downsampling and upsampling by $D < M$, i.e. M / D oversampled subbands; and length L analysis, synthesis filters for the mth subband given by $\mathbf{f}_m = \begin{bmatrix} f_{m,0} & \cdots & f_{m,L-1} \end{bmatrix}^T$, $\mathbf{g}_m = \begin{bmatrix} g_{m,0} & \cdots & g_{m,L-1} \end{bmatrix}^T$ respectively. We also assume in the target tracking application, that the 9 states are indexed by i.

In order to perform Kalman filtering in subbands we derive the relevant equations in four steps:

1) Analysis filter and downsample fullband measurements into subband measurements
2) Compute subband versions of $\mathbf{\Phi}$, **Q**, **H**, $\mathbf{R}_c$ and initialize subband state vector and state error covariance.
3) Compute subband outputs using subband Kalman filter with subband inputs.
4) Upsample and synthesis filter subband outputs to construct fullband outputs.

2.3 Analysis of the Inputs

Analysis or subband decomposition of the measurement vector is performed as follows. We form a time-series for each measurement vector as in Figure 2.

$$\begin{aligned}
\mathbf{y}(k) &= [\,y_1(k) \quad y_2(k) \quad \ldots \quad y_9(k)\,] \\
\mathbf{y}(k-1) &= [\,y_1(k-1) \quad y_2(k-1) \quad \ldots \quad y_9(k-1)\,] \\
\mathbf{y}(k-2) &= [\,y_1(k-2) \quad y_2(k-2) \quad \ldots \quad y_9(k-2)\,] \\
&\vdots \qquad\quad \vdots \qquad\quad \vdots \qquad\quad \vdots
\end{aligned}$$

Figure 2: Time series formation for each measurement.

Thus we define the time series for each fullband measurement with the following notation

$$\begin{aligned}
\mathbf{y}_1(Dk) &= \left[y_1(Dk) \quad \cdots \quad y_1(Dk-L+1)\right]^T \\
\mathbf{y}_2(Dk) &= \left[y_2(Dk) \quad \cdots \quad y_2(Dk-L+1)\right]^T \\
&\vdots \\
\mathbf{y}_9(Dk) &= \left[y_9(Dk) \quad \cdots \quad y_9(Dk-L+1)\right]^T
\end{aligned} \tag{3}$$

Subband decomposition of the measurement vector is computed by analysis filtering the time series for each state and downsampling by D. Therefore we have as the mth subband measurement for the ith state at k (downsampled time scale)

$$w_{i,m}(k) = \mathbf{f}_m^H \mathbf{y}_i(Dk) \tag{4}$$

where

$$\mathbf{y}_i(Dk) = \left[y_i(Dk) \quad y_i(Dk-1) \quad \cdots \quad y_i(Dk-L+1)\right]^T. \tag{5}$$

The mth subband measurement vector is then given by

$$\mathbf{w}_m(k) = \left[w_{1,m}(k) \quad \cdots \quad w_{9,m}(k)\right]^T. \tag{6}$$

In a similar way we can show the following about the remaining inputs to the subband Kalman filter.

The transition matrix for the mth subband $\mathbf{\Phi}_m$ is given by

$$\mathbf{\Phi}_m = \mathbf{\Phi}^D \tag{7}$$

where Φ is the fullband transition matrix and D is the downsampling factor.

The subband noise covariance associated with subband transition matrix $\mathbf{Q}_m$ is given by

$$\mathbf{Q}_m = \mathbf{f}_m^H \mathbf{f}_m \mathbf{Q} \tag{8}$$

where $\mathbf{Q}$ is the fullband noise covariance associated with fullband transition matrix Φ. Note we have assumed that the process noise samples are zero mean, white (uncorrelated), and Gaussian.

The observation matrix for the mth subband, $\mathbf{H}_m$ is given by

$$\mathbf{H}_m = \mathbf{H} \tag{9}$$

where $\mathbf{H}$ is the fullband observation matrix. Note that in this calculation, we have assumed rows of $\mathbf{H}$ contain only one non-zero element and thus do not involve a coupling of state elements in the measurement model. This is the case for target tracking given the measurement equation

$$\mathbf{y}(k+1) = \mathbf{H}\mathbf{x}(k) + \mathbf{v}(k) \tag{10}$$

and observation matrices for range and azimuth

$$\mathbf{H}_R = \begin{bmatrix} 1 & 0 & 0 \\ 0 & 1 & 0 \end{bmatrix}, \mathbf{H}_\theta = \begin{bmatrix} 1 & 0 & 0 \end{bmatrix}. \tag{11}$$

Finally, the subband noise covariance associated with subband observation matrix $\mathbf{R}_{c,m}$ is given by

$$\mathbf{R}_{c,m} = \mathbf{f}_m^H \mathbf{f}_m \mathbf{R}_c \tag{12}$$

where $\mathbf{R}_c$ is the fullband noise covariance associated with fullband observation matrix $\mathbf{H}$. Note we have assumed that the noise samples are white, zero mean, and Gaussian.

In summary, given a time-series for each measurement and fullband Kalman filter inputs, the subband versions of the inputs to the subband Kalman filter are given in Table 1.

Table 1: Subband Kalman Filter Inputs

***m*th Subband Input**	**Notation**	**Equation**
Measurement Vector	$\mathbf{w}_m$	(4)
Transition matrix	$\mathbf{\Phi}_m$	(7)
Noise covariance associated with transition matrix	$\mathbf{Q}_m$	(8)
Observation matrix	$\mathbf{H}_m$	(9)
Noise covariance associated with observation matrix	$\mathbf{R}_{c,m}$	(12)

2.4 Synthesis of the Outputs

Synthesis or reconstruction of the state estimate is performed as follows. We will form a time-series for each subband state estimate as in Figure 3.

$$\begin{aligned}
\hat{\mathbf{u}}_m(k \mid k) &= [\,\hat{u}_{1,m}(k \mid k) \quad \hat{u}_{2,m}(k \mid k) \quad \ldots \quad \hat{u}_{9,m}(k \mid k)\,] \\
\hat{\mathbf{u}}_m(k-1 \mid k-1) &= [\,\hat{u}_{1,m}(k-1 \mid k-1) \quad \hat{u}_{2,m}(k-1 \mid k-1) \quad \ldots \quad \hat{u}_{9,m}(k-1 \mid k-1)\,] \\
\hat{\mathbf{u}}_m(k-2 \mid k-2) &= [\,\hat{u}_{1,m}(k-2 \mid k-2) \quad \hat{u}_{2,m}(k-2 \mid k-2) \quad \ldots \quad \hat{u}_{9,m}(k-2 \mid k-2)\,] \\
&\vdots \qquad\qquad\quad \vdots \qquad\qquad\quad \vdots \qquad\qquad\quad \vdots
\end{aligned}$$

Figure 3: Subband time series formation for each state estimate.

Thus we define the time series for each state estimate in subband m (on the downsampled time-scale) with the following notation

$$\begin{aligned}
\hat{\mathbf{u}}_1(k+1 \mid k+1) &= \left[\hat{u}_{1,m}(k+1 \mid k+1) \quad \cdots \quad \hat{u}_{1,m}(k-L+1 \mid k-L+1)\right]^T \\
\hat{\mathbf{u}}_2(k+1 \mid k+1) &= \left[\hat{u}_{2,m}(k+1 \mid k+1) \quad \cdots \quad \hat{u}_{2,m}(k-L+1 \mid k-L+1)\right]^T \\
&\vdots \\
\hat{\mathbf{u}}_9(k+1 \mid k+1) &= \left[\hat{u}_{9,m}(k+1 \mid k+1) \quad \cdots \quad \hat{u}_{9,m}(k-L+1 \mid k-L+1)\right]^T
\end{aligned} \tag{13}$$

Reconstruction of current *i*th state estimate will be computed by *D*-fold upsampling followed by synthesis filtering of the time series for the *i*th state in each subband. The results for all subbands are then summed. We thus have as the current *i*th state estimate

$$\hat{x}_i(k+1|k+1) = \sum_{m=0}^{M-1} \mathbf{g}_m^H \hat{\mathbf{u}}_{i,m}^D(k+1|k+1) \tag{14}$$

where we have assumed

$$\hat{\mathbf{u}}_{i,m}^D(k+1|k+1) = \left[\underbrace{0 \cdots 0}_{(k+1) \bmod D} \quad u_i\left(\left\lfloor \frac{k+1}{D} \right\rfloor \left\| \frac{k+1}{D} \right\| \right) \quad \underbrace{0 \cdots 0}_{D-1} \quad u_i\left(\left\lfloor \frac{k+1}{D} \right\rfloor - 1 \left\| \frac{k+1}{D} \right\| - 1 \right) \quad \cdots \right]^T \tag{15}$$

is *L* x 1. The current state estimate is then

$$\hat{\mathbf{x}}(k+1|k+1) = \left[\hat{x}_1(k+1|k+1) \quad \cdots \quad \hat{x}_9(k+1|k+1) \right]^T. \tag{16}$$

3. RESULTS

Simulations were conducted to evaluate a 16-subband Kalman filter for the 2D-tracking (range and azimuth) of a single target. Target dynamics are governed by

$$\mathbf{x}(k+1) = \Phi \mathbf{x}(k) + \mathbf{Q}(k) \tag{17}$$

where the time-invariant transition and process noise covariance matrices are given by

$$\Phi = \begin{bmatrix} 1 & T & \frac{T^2}{2} \\ 0 & 1 & T \\ 0 & 0 & 1 \end{bmatrix} \tag{18}$$

and

$$\mathbf{Q} = \frac{2\sigma^2}{\tau} \begin{bmatrix} q_{11} & q_{12} & q_{13} \\ q_{12} & q_{22} & q_{23} \\ q_{13} & q_{23} & q_{33} \end{bmatrix} \tag{19}$$

respectively where σ, τ, β are target acceleration variance, maneuver time constant, and reciprocal of the maneuver time constant respectively, and

$$\begin{aligned} q_{11} &= \frac{1}{2\beta^5}\left(1 - e^{-2\beta T} + 2\beta T + \frac{2\beta^3 T^3}{3} - 2\beta^2 T^2 - 4\beta T e^{-\beta T}\right) \\ q_{12} &= \frac{1}{2\beta^4}\left(e^{-2\beta T} + 1 - 2e^{-\beta T} + 2\beta T e^{-\beta T} - 2\beta T - \beta^2 T^2\right) \\ q_{13} &= \frac{1}{2\beta^3}\left(1 - e^{-2\beta T} - 2\beta T e^{-\beta T}\right) \\ q_{22} &= \frac{1}{2\beta^3}\left(4e^{-\beta T} - 3 - e^{-2\beta T} + 2\beta T\right) \\ q_{23} &= \frac{1}{2\beta^2}\left(e^{-2\beta T} + 1 - 2e^{-\beta T}\right) \\ q_{33} &= \frac{1}{2\beta}\left(1 - e^{-2\beta T}\right) \end{aligned} \tag{20}$$

The state vector represents the position, velocity, and acceleration of the target at time kT where T is the time between measurements. Range and azimuth filters are coupled, i.e. range and azimuth extrapolation requires estimates of range, range rate, and azimuth estimates [8]. The target is initially positioned at (10000, 40000) with a velocity of 200m/s and an initial heading of $-\pi/2$. At t = 160-164, the target undergoes an acceleration of (13, –13). At t = 200-204, the target undergoes another acceleration of (–13, 13). The measurement equation and matrices for the simulation are given by (10) and (11). The measurement noise vectors $\mathbf{v}_i^T(k)$ in (10) are independent Gaussian noise vectors with constant covariance matrices $\mathbf{R}_\theta = r$

$$\mathbf{R}_R = \begin{bmatrix} r & 0 \\ 0 & r \end{bmatrix}, \tag{21}$$

where r_R = 16192, $r_{\dot{R}} = 163.84$, and r_Φ = 7.6212e–05.

In the simulations, we set the initial states of the target to the first measurements and the initial state error covariance matrix is set equal to the measurement error covariance matrix. Track initiation and deletion procedures are not incorporated in the simulations in order to isolate the performance of the subband Kalman filter.

In the design we assume a 16-subband, 2× oversampled uniform-DFT filter bank. The uniform-DFT filter bank leads to conjugate symmetric subbands thus we need only update the first $M/2$ subbands and take their conjugates as the updates on the remaining half. Figures 4 and 5 illustrate nearly identical range tracks for fullband and subband Kalman filters thus confirming fidelity of the subband method.

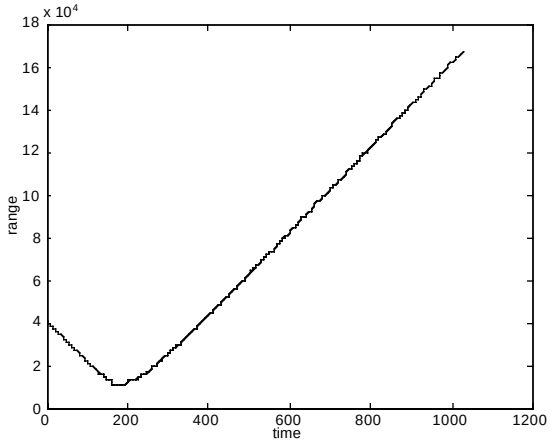

Figure 4: Range track for fullband Kalman filter

Experiment 1 (Selective Updating). In this experiment we examine the effect of updating (i) all subbands, (ii) half the subbands, (iii) only subband #0. Table 2 gives statistics for the mean and standard deviation of $R, \dot{R}, \dot{\theta}$.

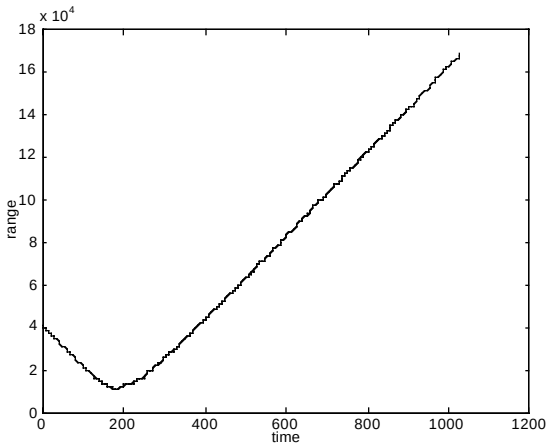

Figure 5: Range track for subband Kalman filter

Table 2: Statistical measures for experiment 1

Statistic	Fullband	Sub (i)	Sub (ii)	Sub (iii)
$\bar{R}$	–7.53e+0	5.33e+0	5.31e+0	5.40e+0
$\bar{\dot{R}}$	–3.18e–1	–3.73e–1	–3.80e–1	–3.76e–1
$\bar{\theta}$	–2.58e–4	–6.89e–4	–6.89e–4	–6.89e–4
σ_R	3.69e+1	5.24e+1	5.13e+1	3.60e+1
$\sigma_{\dot{R}}$	6.50e+0	7.54e+0	7.26e+0	5.68e+0
σ_θ	3.87e–3	8.08e–3	5.22e–3	2.96e–3

We note in case (iii) where only subband #0 Kalman filter is updated, standard deviations are lower than their fullband counterparts but are biased.

Experiment 2 We examine the effect of large measurement noise on the subband Kalman filter when only subband #0 is updated. In (i) we assume 10× and (ii) 100× the noise in Experiment 1.

Table 3: Statistical measures for experiment 2

Statistic	Full (i)	Sub (i)	Full (ii)	Sub (ii)
$\bar{R}$	–2.36e+1	–1.91e+1	–7.30e+1	–6.81e+1
$\bar{\dot{R}}$	–8.26e–1	–6.10e–1	–1.89e+0	–1.24e+0
$\bar{\theta}$	–7.87e–4	–1.72e–3	–2.48e–3	–5.50e–3
σ_R	1.16e+2	8.60e+1	3.49e+2	2.20e+2
$\sigma_{\dot{R}}$	1.51e+1	1.24e+1	3.24e+1	1.67e+1
σ_θ	9.50e–3	5.19e–3	2.29e–2	1.23e–2

Again, we note in subband Kalman filter cases where only the lowest subband is updated, the standard deviations are lower than their fullband counterparts for increased noise.

4. SUMMARY

In this paper we have presented the relations of subband Kalman filter inputs and outputs to the fullband equivalent. We have also presented results from the target-tracking application which demonstrate the subband implementation performs better (in terms of error variance) than the fullband case when 1) only subband Kalman filters with significant energy are updated and/or 2) when the measurement noise is large. These results indicate that the subband method can provide equal or better performance with potentially less computation and/or noisier sensors.

5. REFERENCES

[1] P. P. Vaidyanathan, *Multirate Systems and Filter Banks*. Englewood Cliffs, NJ: Prentice-Hall, 1993.

[2] S. G. Mallat, "A Theory for Multiresolution Signal Decomposition: The Wavelet Representation," *IEEE Transactions on Pattern Analysis and Machine Intelligence*, Vol. 11, No. 7, pp. 674--693, 1989.

[3] L. Hong, "Multiresolutional Distributed Filtering," *IEEE Transactions on Automatic Control*, Vol. 39, No. 4, pp. 853-856, 1994.

[4] L. Hong, "Multiresolutional Multiple-Model Target Tracking", *IEEE Transactions on Aerospace and Electronic Systems*, Vol. 30, No. 2, pp. 518-524, April 1994.

[5] L. Hong and T. Scaggs, "Real-Time Optimal Filtering for Stochastic Systems With Multiresolutional Measurements," *Systems & Control Letters*, Vol. 21, No. 5, pp. 381-387, 1993.

[6] L. Hong, "Two-Level JPDA-NN and NN-JPDA Tracking Algorithms," Proc. of 1994 American Control Conference, pp. 1057-1061, Baltimore, MD, June 1994.

[7] P. De Leon, "On the use of filter banks for parallel signal processing," *7th NASA Symposium on VLSI Design* 1997.

[8] S. Blackman, *Multiple-Target Tracking with Radar Applications*, Artech House 1986.

[9] L. Scharf, *Statistical Signal Processing*, Addison-Wesley, Reading, MA, 1991.

[10] L. Hong, G. Wang, M. Logan and T. Donohue, "Multirate Interacting Multiple Model Filtering for Target Tracking," submitted to *IEEE Transactions on Automatic Control.*